JOURNAL OF MATERIALS SCIENCE 30 (1995) 1217–1224

Electrode configurations and impedance spectra of cement pastes

S. J. FORD, T. O. MASON, B. J. CHRISTENSEN, R. T. COVERDALE*, H. M. JENNINGS
Department of Materials Science and Engineering and Center for Advanced Cement-Based Materials, Northwestern University, Evanston, IL 60208, USA

E. J. GARBOCZI
National Institute of Standards and Technology and Center for Advanced Cement-Based Materials, Building Materials Division, Gaithersburg, MD 20899, USA

Electrode effects on impedance spectra of cement pastes were investigated by two-, three-, and four-point measurements without a potentiostat over the frequency range 0.01 Hz–10 MHz. Electrode immittance effects arising from highly resistive/capacitive contacts cannot be fully corrected by nulling procedures. Two-point measurements are much more susceptible to such effects than three- or four-point measurements. The three- and four-point results on pastes suggest that there is negligible high-frequency "offset" resistance, and that bulk paste arcs are not significantly depressed below the real axis in Nyquist plots. The important impedance-derived equivalent circuit parameters are bulk resistance and capacitance; offset resistance and arc depression angle may not be physically meaningful parameters. Whereas all electrode configurations give reliable values of bulk paste resistance, only the three-point configuration provides the total paste/electrode dual arc spectrum involving a single electrode. Multielectrode (three- or four-point) measurements may be necessary to establish the true bulk paste dielectric constant.

1. Introduction

A typical impedance spectrum of a young cement paste with embedded iron electrodes is given in Fig. 1a and b [1]. Key features are R_e, the electrode resistance, R_b, the bulk paste resistance, R_0, the offset resistance, and ν_{top}, the frequency at the top of the bulk arc. In addition, the angle, θ, describes the depression of the bulk arc below the real axis. Elsewhere [1], we have described how R_b relates to paste microstructure and important engineering parameters (diffusivity and permeability) and how the effective dielectric constant can be calculated knowing ν_{top} and R_b. The dielectric constant is also a strong function of the microstructure [1]. The present work addresses the parameters θ and R_0 as determined by impedance spectroscopy (IS) in two-, three-, and four-point electrode configurations.

To date, all IS of cement pastes has been carried out in the two-point configuration without a potentiostat [1–14]. (Numerous additional studies of iron electrodes in three- and four-point configurations may be found in the corrosion literature, under potentiostatic control; these will not be reviewed here.) Beginning with the pioneering work of McCarter and co-workers [2–4], there have been several studies showing little or no resistance offset and small arc depression angle [2–7]. On the other hand, there have been numerous works showing appreciable resistance offsets and larger arc depression angles, including later work by McCarter and Brousseau [8], work by ourselves [1, 5, 9, 10], and extensive works by Beaudoin and co-workers [11–14]. Negligible resistance offset and smaller depression angle are apparently associated with larger bulk paste resistance, e.g. due to silica fume additions.

There have been several attempts in the literature to explain the microstructural origins of the individual bulk arc features in Fig. 1. Beaudoin and co-workers [6, 11–16] have argued persuasively that R_0 is due to the capillary pore phase and is inversely related to its volume fraction and conductivity. They also claimed that the bulk arc diameter in Fig. 1b, R_2, is due to solid/liquid interfaces, and is proportional to interface thickness, the number of such interfaces, and inversely proportional to the interfacial conductivity. (The number of solid/liquid interfaces was claimed to be inversely proportional to the volume fraction of capillary pores and the mean pore size.) We have

*Present address: Master Builders, Inc., 23700 Chagrin Boulevard, Cleveland, OH 44122, USA.

0022–2461 © 1995 Chapman & Hall

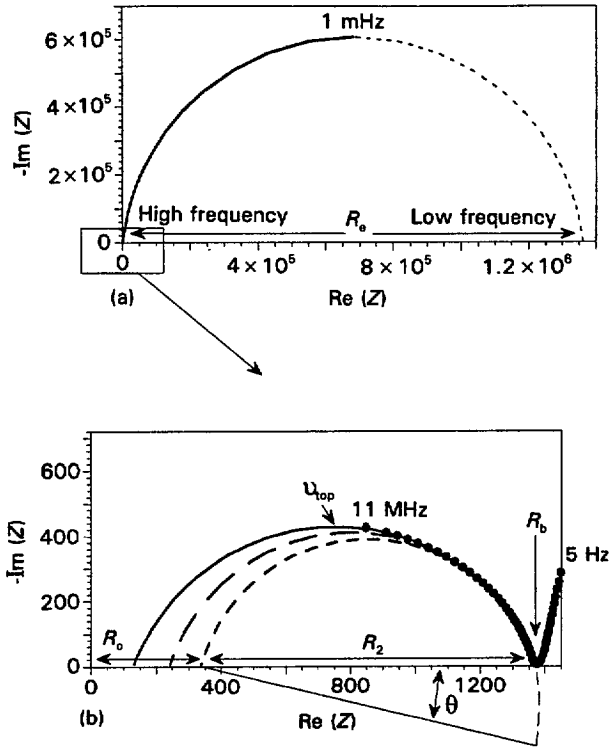

Figure 1 (a) Typical two-point impedance spectrum for the Opc/steel system (w/c = 0.4, 12 days, 10 cm × 2.7 cm × 3.6 cm bar). (——) Experimental data obtained between 11 MHz and 1 mHz, (· · ·) simulations to 10 μHz. (b) Enlargement of high-frequency range showing the uncertainty in R_0 associated with fits to different frequency limits of the experimental data: (-·-·-) up to 3 MHz, (—·—) up to 6 MHz, (——) up to 11 MHz. (After [1].)

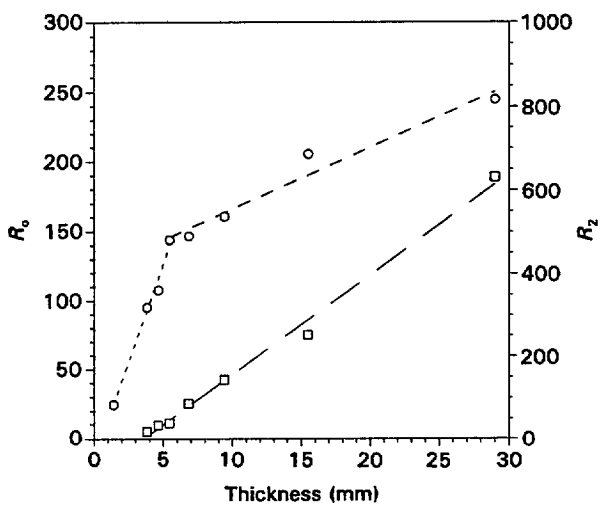

Figure 2 Plots of (○) R_0 and (□) R_2 from Xie *et al.* [14] versus interelectrode spacing on the Opc/steel system (w/c = 0.30, 3 months) in two-point configuration.

reproduced the recent results of the Beaudoin group [14] in Fig. 2, showing discontinuities in R_0 and R_2 versus paste thickness in the vicinity of 5 mm. This was attributed to changes in pore fluid conductivity in thin specimens. Additionally, Beaudoin and co-workers suggested that the bulk arc depression angle is proportional to the distribution of pore sizes in the paste, i.e. the wider the distribution, the larger the depression angle [12, 17].

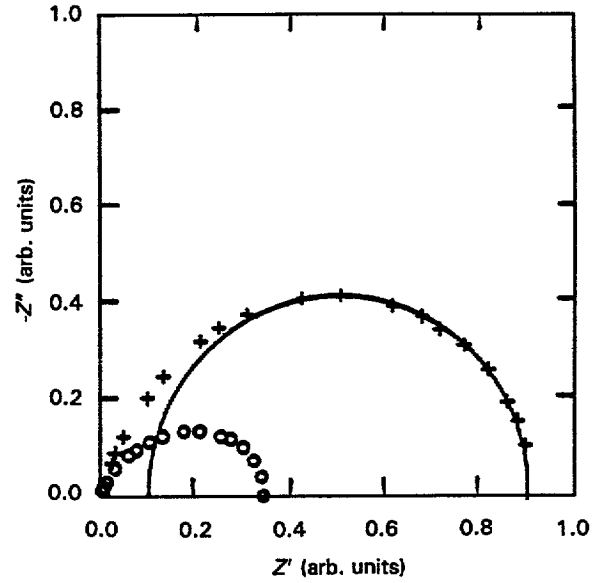

Figure 3 Computer-simulated impedance spectra for a 100 × 100 × 100 pixel cement paste system at w/c = 0.4, showing R_0- and R_2-like features. α = degree of hydration: (○) 0.505, (+) 0.650. (After [19].)

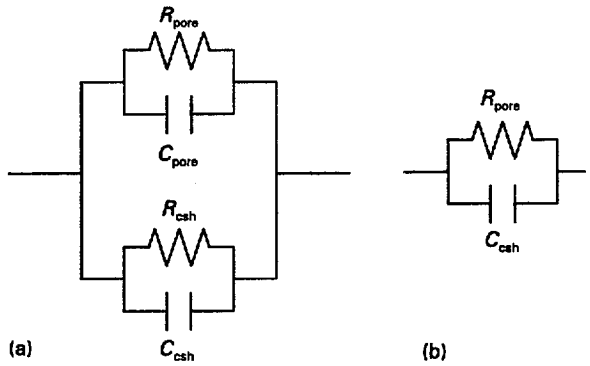

Figure 4 (a) Equivalent circuit model for a 3–3–0 pore phase–CSH–cement, $Ca(OH)_2$ composite, which reduces to (b) if $R_{pore} \ll R_{csh}$ and $C_{pore} \ll C_{csh}$.

On the other hand, we have pursued a digital image-based computer model of the evolving microstructure, combined with a resistor/capacitor network model to predict the impedance response [18–20]. This work suggests that R_0 is an artefact of fitting only the low-frequency side of the bulk arc, which can have the appearance of two overlapping arcs as in Fig. 3. True series behaviour, i.e. completely separated arcs, is only obtained in two-dimensional simulations where both capillary pores and CSH gel are depercolated. In reality, depercolation of the capillary pore system does not occur in cement pastes until extremely high degrees of hydration.

Intuitively, we can consider cement paste to be a 3–3–0 electrocomposite, where the numbers refer to the interconnectivity of the highly conductive pore phase (three-dimensional), the less conductive CSH product phase (three-dimensional), and the highly resistive cement grains and/or $Ca(OH)_2$ product (zero-dimensional). Neglecting the cement grains and $Ca(OH)_2$, we can consider paste to have the equivalent circuit model in Fig. 4a, which should reduce to

the simple RC circuit in Fig. 4b under the assumptions that $R_{pore} \ll R_{csh}$ and $C_{pore} \ll C_{csh}$. The result should be a single IS arc.

2. Experimental procedure

Type I ordinary Portland cement (OPC) was mixed with distilled water in a Hobart planetary mixer for 15 min at low speed. The mix was cast in plexiglas moulds into bars 2.54 cm × 2.54 cm × 10 cm for multipoint measurements and a series of bars with 2.54 cm × 2.54 cm cross-section and various lengths for parallel two-point measurements. Outer electrodes of low-carbon iron (to simulate cement/rebar interfaces) with an area of 2.5 cm^2 were cast in place towards the ends of multipoint and two-point specimens, perpendicular to the long axis of the bar. Experience showed that whereas planar contacts were desirable for "excitation" electrodes (X_{hi}, X_{lo}), point contacts gave the best results for "sensing" (S_{hi}, S_{lo}) contacts. Plate or wire-wrap electrodes led to undesirable inductive effects due to their interference with the response of the specimen. Sensing contacts were made of sharp points of copper wire pressed into the surface of multipoint bars with plexiglas jigs and c-clamps. Specimens were cured at 100% relative humidity in a humidity chamber fixed to the front of the impedance analyser.

The impedance analyser employed was a Schlumberger 1260 in true four-point mode. The use of a potentiostat limits the upper frequency to between 10 and 100 kHz, above which the analyser measures the response of the potentiostat rather than the specimen. Because we were interested in the bulk paste response which is in the 100 kHz–10 MHz range, no potentiostat was used. The 1260 was operated in the floating, differential input mode, with individual coaxial cables connected to the front panel (Gen Out = X_{hi}, V1(hi) = S_{hi}, V1(lo) = S_{lo}, Current In = X_{lo}) with all outers shorted together (but not grounded) by means of a brass plate located as close as possible to the front panel of the unit. To minimize cable immittance contributions, cables running from the brass plate to the specimen were kept as short as possible. This was dictated by the maximum interelectrode spacing, i.e. 10 cm. Connections were made between the coaxial centre leads and the electrodes by means of small alligator clips. Connections for two-, three-, and four-point measurements are shown in Fig. 5a. Excitation amplitudes were kept as small as possible, 20 mV, to minimize inductive effects. A nulling procedure was employed to correct for lead and connector immittances. Each spectrum was repeated with no sample (open) and also with shorted leads (shorted). Corrections were made using either the built-in 1260 null-correction, or with our own software using the procedure given elsewhere [1].

It must be pointed out that it is impossible to perform null-corrections at the sample surface, i.e. beneath the electrodes. The reason for this is illustrated in Fig. 5b, which is an equivalent circuit model of the four-point bar in Fig. 5a. When the sample (represented by R_s, C_s circuits inside the inner box) is removed, the various electrode circuits (represented by R_e, C_e circuits in the outer box) are simultaneously removed. "Shorting" therefore involves replacing the outer box with a short circuit rather than the inner box, as desired. This has a major effect on the corrected spectra, as we will demonstrate. Null corrections at the true surface of the sample, i.e. the inner box, are impossible.

In order to test the effect of external nulling (outer box of Fig. 5b) versus internal nulling (inner box of Fig. 5b), we constructed the simplified circuit in Fig. 6 using resistors and capacitors. All electrode resistances and capacitances were made identical, but were orders of magnitude larger than the bulk resistance

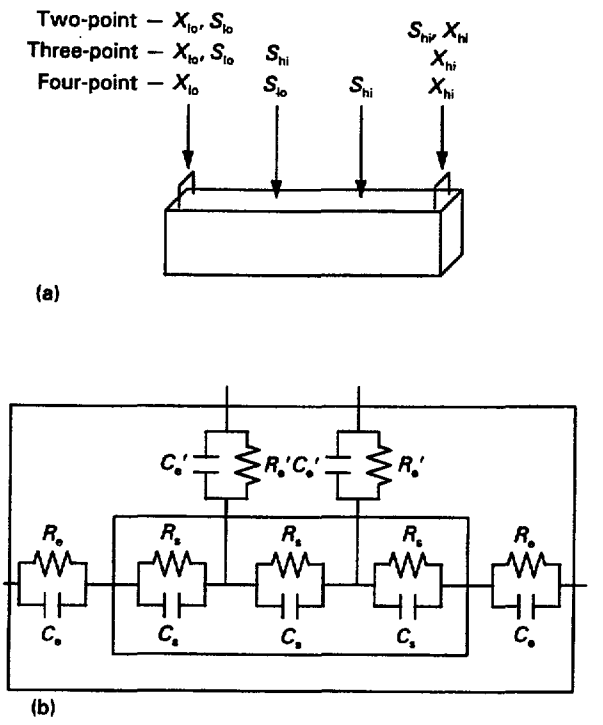

Figure 5 (a) Electrode connections for IS measurements, and (b) equivalent circuit for four-point connections.

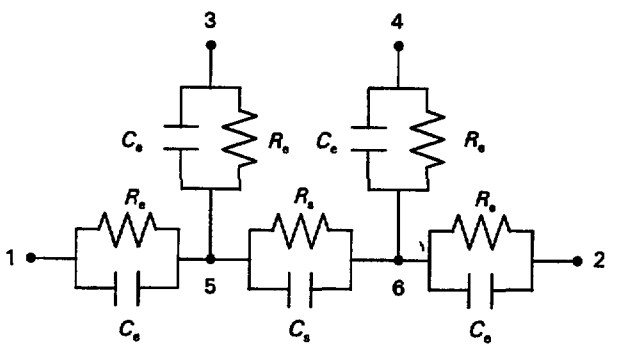

	X_{lo}	S_{lo}	S_{hi}	X_{hi}
Two-point	1	1	2	2
Three-point	1	1	4	2
Four-point	1	3	4	2

Figure 6 Schematic drawing of resistor–capacitor network simulating cement/steel behaviour with two-, three-, and four-point connections as shown. $R_S = 50.0\,\Omega$, $C_S = 1.5$ nF, $R_e = 100$ KΩ, $C_e = 10\,\mu$F.

TABLE I "Bulk" arc frequencies

Figure	Config.	L (cm)	Frequency[a] (max) (MHz)	(top) (MHz)	(min) (Hz)
7	4	3	10.00	0.79	200
	3	7	6.31	1.59	1995
	2	9	3.98	2.51	19953
8a	Sim		10.00	2.10	50119
	4		7.94	1.99	158
	3		3.98	1.58	31623
	2		3.16	1.26	50119
8b	Sim		10.00	2.10	50119
	4		10.00	1.99	158
	3		10.00	1.99	25119
	2		6.31	1.99	39811
8c	Sim		10.00	2.10	50119
	4		10.00	1.99	25
	3		10.00	1.99	2512
	2		10.00	1.99	3162
9a	2	4	6.31	3.16	6310
	2	6	6.31	3.16	3162
	2	8	6.31	3.16	3162
9b	2	5	6.31	3.16	3162
	2	7	6.31	3.16	3162
9c	4	4	10.00	0.32	794
	4	6	10.00	0.25	1000
	4	8	10.00	0.25	501
9d	4	5	10.00	0.25	501
	4	7	10.00	0.20	1259

[a] Freq. (max) = frequency corresponding to the left-most point of the impedance arc.
Freq. (top) = frequency at the top of the impedance arc.
Freq. (min) = frequency of the impedance arc where $-\mathrm{Im}(Z)$ is at a minimum.

and capacitance, respectively. The values were chosen to emulate the actual bulk and electrode values for a young OPC paste/iron electrode system. Excitation and sensing leads were connected as shown. Null corrections were made by external shorting (contacts 1–4) and also by internal shorting (contacts 5, 6).

Impedance spectra of pastes and simulated circuits were plotted and analyzed in Nyquist format by a commercially available software program [21]. To avoid clutter in the impedance spectra, frequencies corresponding to the left (frequency max), top (frequency top), and right (frequency min) of each bulk arc are given in Table I.

3. Results

A comparison of null-corrected two-, three-, and four-point spectra on a 17 h old OPC paste bar is given in Fig. 7. The interelectrode spacings were different because the two-point spacing was fixed by the cast in-place iron electrodes (9 cm), whereas the interelectrode spacing of the three- and four-point electrodes were adjustable but had to be less than 9 cm. In spite of the different spacings, the bulk resistances scale appropriately with length. There is a noticeable difference, however, between the two-point spectrum,

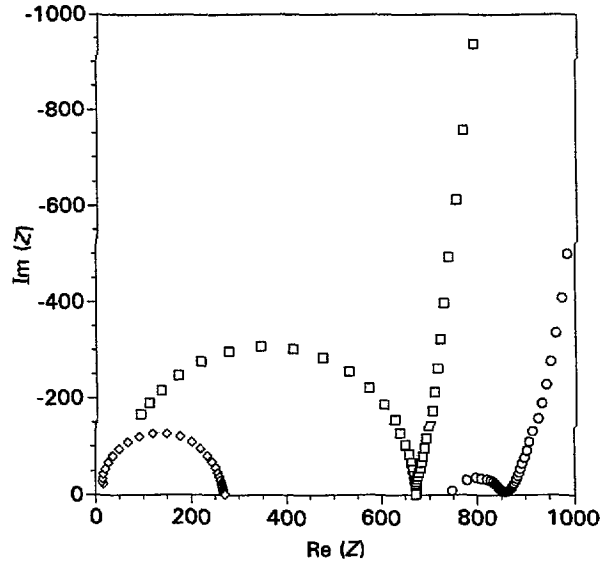

Figure 7 Comparison of (○) two-, (□) three-, and (◇) four-point impedance spectra for a 17 h old Opc/steel system with w/c = 0.4. L: (○) 9 cm, (□) 7 cm, (◇) 3 cm. (Frequency values in Table I.)

exhibiting arc depression and a large offset resistance, and the multipoint spectra, which are nearly semicircular with no apparent offsets.

To establish a possible origin for the anomalous behaviour of the two-point spectrum, we performed IS experiments on the resistor–capacitor network of Fig. 6. Raw data are plotted in Fig. 8a and data for external and internal null corrections are plotted in Fig. 8b and c, respectively. In each case the "simulated" spectrum was calculated by the "Equivalent Circuit" software [21] knowing the correct values of the resistors and capacitors used. The raw data exhibit large deviations, particularly so for the two-point configuration. More significantly, the deviations cannot be fully corrected by "external" nulling (Fig. 8b). This problem is most severe for two-point measurements. Only when "internal" nulling is employed do we obtain good agreement between two-, three-, and four-point spectra and the spectrum calculated on the basis of the known R/C values (Fig. 8c).

We also examined an 8 day old OPC paste for IS response in two-point versus four-point configurations as a function of interelectrode spacing. Results are shown in Fig. 9. The four-point measurements were on a single bar, whereas to replicate the same interelectrode spacings, five different two-point specimens were simultaneously cast from the same mix as used for the four-point bar. Again, in spite of null-corrections, the two-point spectra (Fig. 9a and b) are deformed and significantly depressed below the real axis. Furthermore, they exhibit sizeable offset resistances. In contrast, the four-point spectra (Fig. 9c and d) are nearly perfect semicircles centred on the real axis and passing through or very near to the origin. The bulk resistances (the low-frequency intercept of the bulk arc) agreed well between the two- and four-point spectra; resistivities agreed to within 5% independent of configuration or interelectrode spacing.

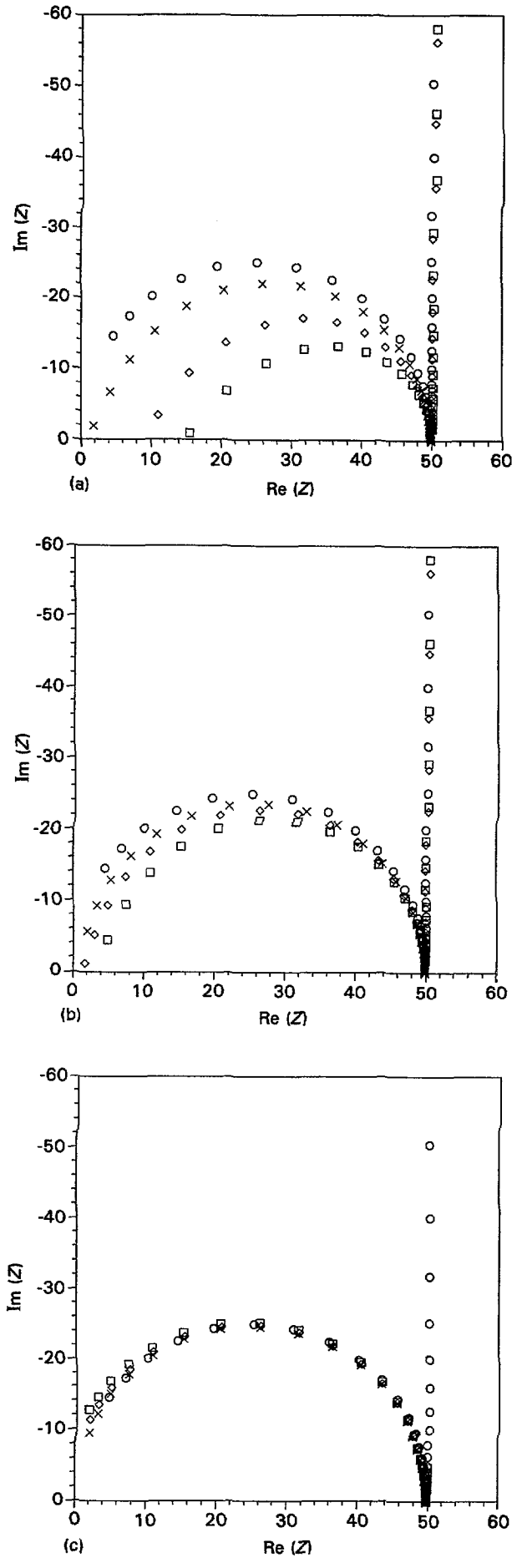

Figure 8 (a) Raw, (b) "externally" null-corrected, and (c) "internally" null-corrected IS curves versus (○) expected (simulated) behaviour calculated on the basis of the known resistors and capacitors in Fig. 6: (□) two-point, (◇) three-point, (×) four-point. (Frequency values in Table I.)

4. Discussion

The inability to fully correct IS data collected on resistor–capacitor networks using "external" versus "internal" nulling (see Figs 5, 6 and 8) suggests one possible explanation for the severe arc depression and offset resistance in two-point versus multipoint IS measurements. Upon removing the steel or copper *electrodes from a cement paste, high resistance and* capacitance contacts are simultaneously removed. It is therefore impossible to null-correct at the specimen surface. Apparently, two-point measurements are considerably more susceptible to such effects than multipoint measurements when dealing with cement pastes (see Figs 7 and 9).

Fortunately, this has little effect on bulk resistance determination. In Fig. 10a the offset, R_0, and arc diameter, R_2, from the two-point data in Fig. 9 are plotted versus interelectrode spacing. Also plotted are the sum of these two values ($R_b = R_0 + R_2$) alongside the four-point bulk resistance, R_b, from Fig. 9. The agreement is excellent. In Fig. 10b, the sum of $R_0 + R_2$ from the data of Xie *et al.* [14] in Fig. 2 is similarly plotted versus interelectrode spacing. The behaviour is linear and passes through the origin. We conclude that the discontinuities in R_0 and R_2 in Fig. 2 are due to increased distortion of two-point arcs at small interelectrode spacings. In spite of this, $R_b = R_0 + R_2$, remains a valid measure of bulk resistance. Given the relative ease and good reproducibility of two-point measurements, we recommend the use of this configuration *for bulk resistance measurements.*

Measurements of electrode properties, on the other hand, can be made in either two- or three-point configurations. Because lower frequencies are employed, null corrections are not required to obtain reliable values. It should be pointed out, however, that the three-point configuration allows for a single electrode to be studied. In contrast, the electrode arc in a two-point spectrum is really a convolution of two arcs, one from each electrode. The three-point measurement is the configuration of choice to examine bulk and electrode arcs simultaneously. (Measurements to even lower frequencies than in Figs 7 and 9 are possible with the 1260; a nearly complete electrode arc results as in Fig. 1a.)

If a precise bulk electrode arc is to be obtained, a multipoint technique must be employed. Furthermore, a potentiostat should not be used so that IS can be performed up to the megahertz range. It should be cautioned that there are often reproducibility problems and potential distortions associated with multipoint techniques. We suspect that these arise due to asymmetry in the sensing electrode resistances/ *capacitances and/or asymmetry in the placement of* the sensing electrodes along the specimen. We occasionally see bulk arcs shifting into the negative imaginary-negative real quadrant in three- and four-point configurations, particularly so for interelectrode spacings of 1 cm or less. Because these distortions occur in the megahertz range, there is also the possibility of interelectrode interference at close spacings (S_{hi} versus S_{lo}, and also S_{hi} versus X_{hi}). Extreme care must be taken to collect reproducible data in multipoint

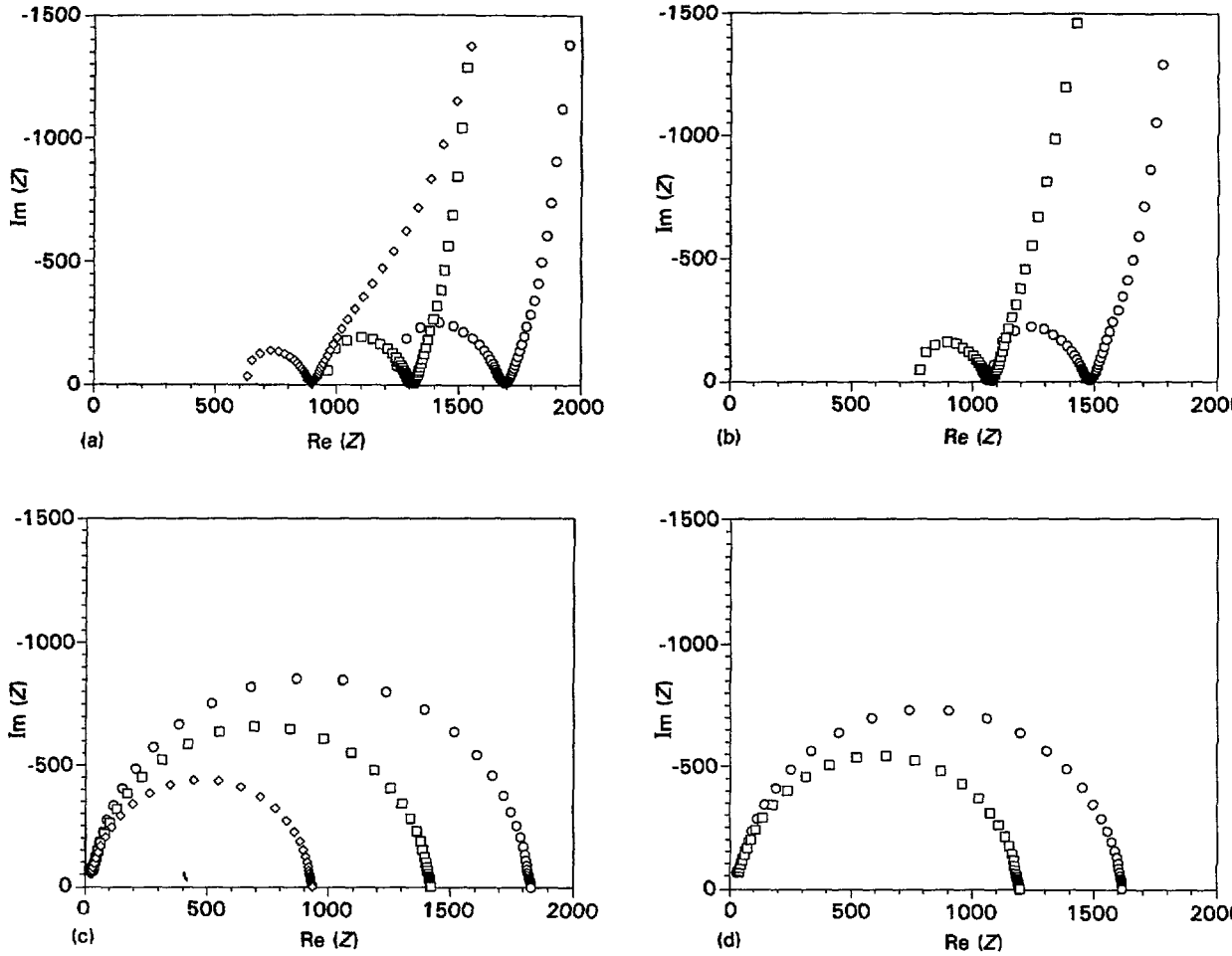

Figure 9 (a, b) Two-point impedance spectra versus interelectrode spacing, and (c, d) four-point impedance spectra versus interelectrode spacing for 8 day old Opc/steel samples with w/c = 0.4. (a, c) L = (○) 8, (□) 6, (◇) 4 cm. (b, d) L = (○) 7, (□) 5 cm. (Frequency values in Table I.)

configurations. Parallel experiments on resistor–capacitor networks are recommended.

In order to ascertain how accurately IS can be used to establish dielectric constants of cement pastes, we have used "Equivalent Circuit" [21] to extract capacitances from the R/C circuit experiments of Fig. 8; results are shown in Fig. 11a. Because of arc distortion and depression, fits were obtained using the equivalent circuit in Fig. 11b, where the capacitor is replaced by a constant phase element. In the case of three- and four-point spectra, the offset resistance was negligibly small. Spectra were fit to the maximum frequency of 1.5 MHz. The CPE capacitances shown vary with the electrode configuration and the type of null-correction employed. (The true value of capacitance was measured to be 1.5 nF.) It is obvious that two-point spectra overestimate the capacitance, particularly so if no null-corrections are performed. Furthermore, "external" null corrections result in as much as a 40% error in the case of the two-point spectrum. This error is significantly less for three-point and four-point configurations. Only with "internal" nulling did the two-, three-, and four-point capacitance values agree with the true value. The extent of null-correction errors obviously depend upon the RC time constants of the circuit elements involved. A more extensive treatment of the effect of such errors on the determination of dielectric constants in cement pastes will be given elsewhere.

A major ramification of the present study relates to microstructure–property relationships in cement pastes. Our work to date is far from exhaustive, but we observe little or no bulk offset resistance in multipoint impedance spectra of cement pastes (see Figs 7 and 9). If this is confirmed in future studies, models incorporating a series equivalent circuit element corresponding to a resistance offset will need to be carefully re-examined. In addition, we find little, if any, arc depression of the bulk arc in multipoint experiments. As pointed out in the introduction, we and others have interpreted the arc depression in two-point spectra as arising from a distribution to pore sizes. This interpretation may be unwarranted if arc depression can be shown to be an experimental artefact rather than a microstructural phenomenon.

5. Conclusion

The inability to completely null-correct impedance spectra is the probable cause of offset resistance and arc depression in two-point impedance spectra of cement pastes with steel electrodes. In contrast, multipoint (three- and four-point) measurements show a nearly perfect bulk paste arc, centred on the real axis

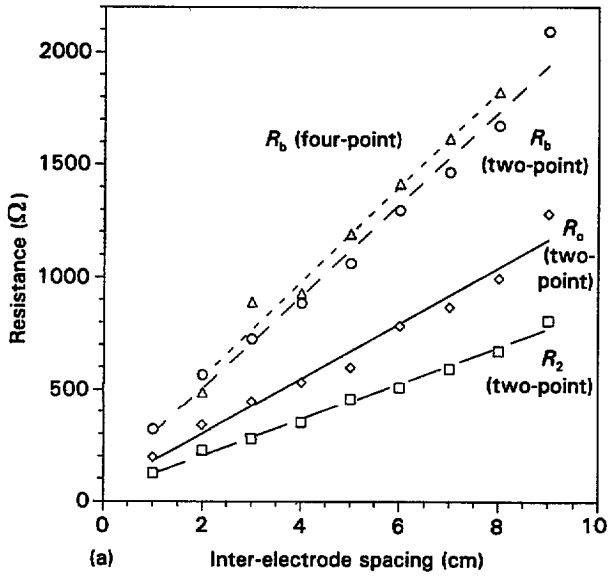

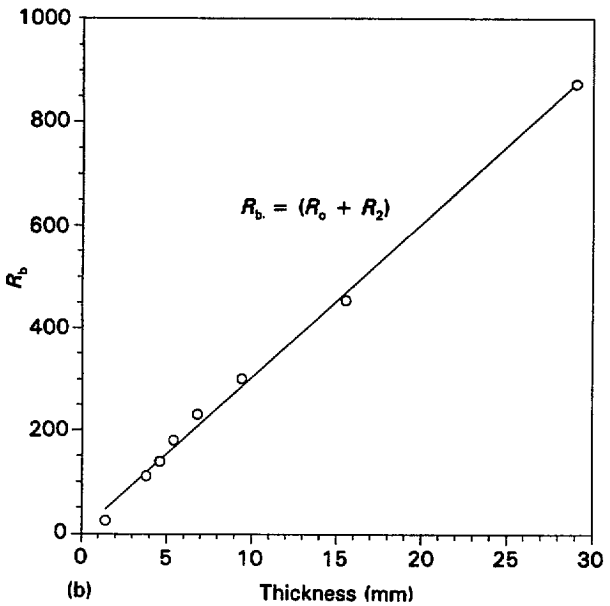

Figure 10 (a) Resistance versus interelectrode spacing from Fig. 9. The sum of two-point offset and arc diameter agrees well with four-point bulk resistance. (b) The sum of two-point offset and arc diameter from Fig. 2 [14], is linear with interelectrode spacing and passes through the origin.

and passing near or through the origin in Nyquist plots. This experimental artefact in no way influences the electrode arc (in two- and three-point studies) or the value of the bulk resistance (in two-, three-, or four-point spectra). Standard two-point IS is still preferable for bulk resistance measurements, given its simplicity and reproducibility. On the other hand, three-point IS is necessary if a single electrode is to be studied. By eliminating the use of a potentiostat, three-point IS can be employed to simultaneously study the cement paste. Multipoint techniques (three- or four-point IS) are required to obtain a reliable picture of the bulk paste properties such as dielectric constant and arc depression angle. Four-point IS eliminates the electrode arc entirely.

In view of the present results (multipoint spectra showing negligible offset and depression angle) it may

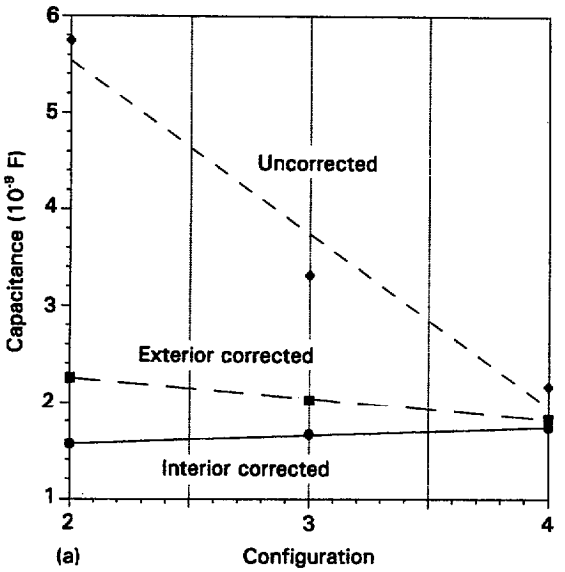

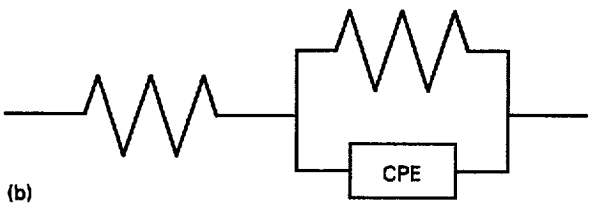

Figure 11 (a) "Equivalent Circuit" [21] fitting of the R/C network experimental data in Fig. 8a, b and c, for the three different configurations, gave these capacitance values. The actual capacitor value was 1.5 nF and the spectra were fit to a maximum frequency of 1.5 MHz. (b) The equivalent circuit employed.

be necessary to re-evaluate existing microstructure-based models of cement paste electrical behaviour.

Acknowledgement

This work was supported by the Science and Technology Center for Advanced Cement-Based Materials under NSF grant no. DMR-91-20002.

References

1. B. J. CHRISTENSEN, R. T. COVERDALE, R. A. OLSON, S. J. FORD, E. J. GARBOCZI, H. M. JENNINGS. and T. O. MASON, *J. Am. Ceram. Soc.* **11** (1994).
2. W. J. McCARTER, *Cem. Concr. Res.* **17** (1987) 517.
3. W. J. McCARTER, S. GARVIN and N. BOUZID, *J. Mater. Sci. Lett.* **7** (1988) 1056.
4. W. J. McCARTER and S. GARVIN, *J. Phys. D Appl. Phys.* **22** (1989) 1773.
5. B. J. CHRISTENSEN and T. O. MASON, *J. Am. Ceram. Soc.* **4** (1992) 939.
6. A. BERG, G. A. NIKLASSON, K. BRATERVIK, B. HEDBERG and L. O. NILSSON, *J. Appl. Phys.* **71** (1992) 5897.
7. Z. XU, P. GU, P. XIE and J. J. BEAUDOIN, *Cem. Concr. Res.* **23** (1993) 1007.
8. W. J. McCARTER and R. BROUSSEAU, *ibid.* **20** (1990) 891.
9. C. A. SCUDERI, T. O. MASON, and H. M. JENNINGS, *J. Mater. Sci.* **26** (1991) 349.
10. B. J. CHRISTENSEN, T. O. MASON and H. M. JENNINGS, *Mater. Res. Soc. Symp. Proc.* **245** (1992) 271.
11. P. GU, P. XIE, J. J. BEAUDOIN and R. BROUSSEAU, *Cem. Concr. Res.* **22** (1992) 833.
12. *Idem, ibid.* **23** (1993) 157.

13. Z. XU, P. GU, P. XIE and J. J. BEAUDOIN, *ibid.* **23** (1993) 853.
14. P. XIE, P. GU, Y. FU and J. J. BEAUDOIN, *ibid.* **24** (1994) 92.
15. P. GU, Z. XU, P. XIE and J. J. BEAUDOIN, *ibid.* **23** (1993) 531.
16. P. XIE, P. GU, Z. XU and J. J. BEAUDOIN, *ibid.* **23** (1993) 359.
17. P. GU, P. XIE, Y. FU and J. J. BEAUDOIN, *ibid.* **24** (1994) 86.
18. R. T. COVERDALE, E. J. GARBOCZI, H. M. JENNINGS, B. J. CHRISTENSEN and T. O. MASON, *J. Am. Ceram. Soc.* **76** (1993) 1153.
19. R. T. COVERDALE, B. J. CHRISTENSEN, H. M. JENNINGS, T. O. MASON, D. P. BENTZ and E. J. GARBOCZI, *J. Am. Ceram. Soc.*, submitted.
20. R. T. COVERDALE, B. J. CHRISTENSEN, T. O. MASON, H. M. JENNINGS and E. J. GARBOCZI, *J. Mater. Sci.* **29** (1994) 4984.
21. B. A. BOUKAMP, "Equivalent Circuit (EQUIVCRT.PAS)", University of Twente, Department of Chemical Technology, P.O. Box 217, 7500 AE Enschede, The Netherlands (1988).

Received 19 May
and accepted 5 July 1994